Solvent effects on the thermal isomerization of a rotary molecular motor

Lubbe, Anouk S.; Kistemaker, Jos C. M.; Smits, Esther J.; Feringa, Ben L.

Published in:
PPCP : Physical Chemistry Chemical Physics

DOI:
10.1039/c6cp03571j

PCCP

PAPER

View Article Online
View Journal | View Issue

Cite this: *Phys. Chem. Chem. Phys.*, 2016, **18**, 26725

Solvent effects on the thermal isomerization of a rotary molecular motor†

Anouk S. Lubbe,‡ Jos C. M. Kistemaker,‡ Esther J. Smits and Ben L. Feringa*

Received 24th May 2016,
Accepted 2nd September 2016

DOI: 10.1039/c6cp03571j

www.rsc.org/pccp

As molecular machines move to exciting applications in various environments, the study of medium effects becomes increasingly relevant. It is difficult to predict how, for example, the large apolar structure of a light-driven rotary molecular motor is affected by a biological setting or surface proximity, while for future nanotechnology precise fine tuning and full understanding of the isomerization process are of the utmost importance. Previous investigations into solvent effects have mainly focused on the relatively large solvent–solute interaction of hydrogen bonding or polarization induced by the isomerization process. We present a detailed study of a key step in the rotary process *i.e.* the thermal helix inversion of a completely apolar rotary molecular motor in 50 different solvents and solvent mixtures. Due to the relative inertness of this probe, we are able to study the influence of subtle solvent–solvent interactions upon the rate of rotation. Statistical analysis reveals which solvent parameters govern the isomerization process.

Introduction

The term ''solvent effects'' comprises a large range of different solvent–solvent and solvent–solute interactions and is used to describe the combined effect of these interactions on chemical reactivity.[1] Even when the solvent is not participating in the reaction itself, solvent effects can be large and have therefore been studied in detail.[2] As the solvent is such an important part of any chemical reaction, its influence was already extensively studied in the 19th century. Pioneering work in the field was performed among others by Menshutkin,[3] Grunwald and Winstein,[4] Hammett and Deyrup,[5] and Hughes and Ingold,[6] but even after 150 years of extensive research, the nature of solvent effects remains elusive and its study of great importance. Recent examples include solvent effects in catalysis,[7] gelation,[8] regioselectivity in *ortho*-metalation,[9] radical reactions[10] and biomass conversion.[11] In unimolecular reactions, solvent effects are generally smaller but can comprise many different interactions. Therefore, for unimolecular reactions, a solvent scope can be used to gain insight in the effect of various solvent parameters. For example, significant solvent effects have been found in various thermal decomposition reactions,[12,13] ring inversion in cyclohexane,[14] the rotational relaxation of rod-like molecules,[15] and the fluorescence lifetime of rhodamine dyes.[16] The choice of solvent can even lead to different reaction mechanisms, as prominently observed in S_N1/S_N2 reactions,[6] or more recently in a denitrogenation reaction to form housane[17–19] and photodisassociation in guaiacol.[20] Solvent effects on the photoisomerization of stilbene has been studied in detail.[21–23] The results have been explained using Kramers Theory.[24] Kramers theory states that in low-friction (low viscosity) media, the reaction rate increases with increasing friction. In medium-friction media the reaction rate will start to decrease with increasing friction until finally in high-friction media the reaction rate will approach the Smoluchowski limit, an inverse dependency on the solvent viscosity. Additionally, Gegiou *et al.* have argued that based on the free-volume model, this dependency should include a factor α (≤ 1), since only part of a molecule is required to move during an isomerization process.[25,26] This led to the following rate equation (in which η is the viscosity, and β is a fitting parameter):

$$\ln k = \beta - \alpha \ln \eta \quad (1)$$

Related studies have been performed for the photoisomerization of diphenylbutadienes and azobenzenes, which show similar behavior.[22] Additionally, it is suggested that at low viscosities, solvent response frequencies are comparable to the reaction rate and that therefore medium effects other than viscosity may influence the reaction rate.[23,27] Especially in functionalized azobenzenes, a large effect of solvent polarity was observed for both the photochemical and the thermal isomerization.[28,29] For the latter, the influence of polarity on the rate was in fact much larger than the viscosity effect, which can be attributed to the significant change in dipole upon *cis* to

Center for Systems Chemistry, Stratingh Institute for Chemistry and Zernike Institute for Advanced Materials, University of Groningen, Nijenborgh 4, 9747 AG Groningen, The Netherlands. E-mail: b.l.feringa@rug.nl

† Electronic supplementary information (ESI) available: Synthesis and characterization of motor **1**; kinetic experiments; application of the viscosity-correction Eyring equation; fatigue test of motor **1**; viscosity measurements. See DOI: 10.1039/c6cp03571j

‡ These authors contributed equally.

trans isomerization. For example, the rate of the thermal *cis* to *trans* isomerization of an amine functionalized azobenzene was shown to be increased ~9000-fold by switching from cyclohexane to DMF, despite the two having similar viscosities.[28] An investigation of the thermal and photochemical isomerization of bis-oxonols using twenty six different polar solvents showed that the thermal process is less sensitive to viscosity than the photochemical process, and that there is a marked difference in the response to protic and aprotic solvents.[30] Analogous to the observations for azobenzenes, the effect of a certain group of solvents on the thermal isomerization rate was significantly enlarged. For bis-oxonols these are protic solvents, which have a much larger interaction with the solute due to hydrogen bonding.

For molecular motors, studies into solvent effects have so far been limited.[31,32] These compounds are structurally related to stilbenes, and it was indeed proven in a recent example that molecular motors obey the free-volume model.[33] However, opposed to stilbenes, rotary molecular motors readily undergo thermal isomerization. Additionally, none of the configurations a molecular motor can adopt has a significant dipole moment and no polar or hydrogen bonding substituent is required (Scheme 1). These structural properties make molecular motors ideal probes to study solvent effects, as they will not suffer from disproportionally large influences of specific solvents, such as observed for azobenzenes and bis-oxonols. These assumptions concur with the findings of Hicks *et al.*,[34] who conclude that polarity can play a key role in isomerization dynamics, but that this effect is only significant when the process involves a large change in charge distribution. The influence of viscosity on the functioning of a second-generation molecular motor was investigated previously and determined to be large, but since the measurements were performed in only three solvents, no conclusion regarding any other solvent effects was reached.[35] In a recent publication, we have further studied the influence of viscosity on the rate of the thermal isomerization of molecular motors.[36] It was determined that this process can be described using eqn (1) and furthermore, that both α and β are viscosity and temperature dependent. This led to a reformulation of the Eyring equation, from which viscosity-dependent activation parameters could be obtained. However, the solvents in the previous investigation were limited to a range of linear alkanes. It is therefore impossible to reach any definite conclusions regarding solvent effects other than viscosity. Here we present an extensive investigation of the rate of the thermal isomerization of an apolar second generation molecular motor in 50 solvents and solvent mixtures. We aim to gain a deeper understanding regarding the influence of solvent on this thermal isomerization process, especially regarding subtle effects which may have been overlooked in the past due to very large dipole–dipole or hydrogen bonding interactions. To the best of our knowledge, this is the most comprehensive solvent scope ever studied on a unimolecular thermal reaction.

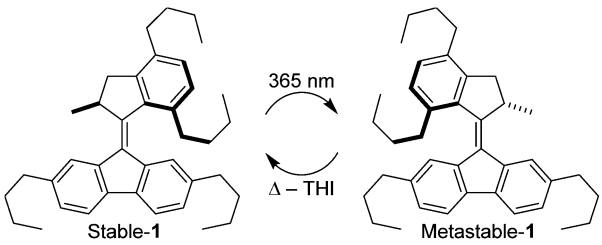

Scheme 1 Structure and isomerization processes of motor **1**. Photochemical *E*–*Z* isomerization using UV-light to metastable-**1** and thermal helix inversion (THI) to stable-**1**.

Results & discussion

The thermal helix inversion of molecular motor **1** was previously used in the study of viscosity effects on unimolecular thermal processes.[36] Its synthesis and characterization can be found in the ESI.† The motor was initially selected because of its *n*-butyl chains, which ensure high solubility in many solvents, and its equal mass balance around the central double bond leading to a similar displacement of both halves during isomerization. Additionally, the motor is apolar in all of its configurations, and during the thermal isomerization step (helix inversion) virtually no polarization is induced.[31] Therefore, we expect motor **1** to be almost inert to solvent–solute interactions, save for London dispersion forces and potentially some π–π stacking. Upon irradiation of motor stable-**1**, photoisomerization at its central double bond occurs, forming a diastereoisomer: metastable-**1**. In this diastereoisomer the stereogenic methyl group has adopted a pseudoequatorial rather than a pseudoaxial orientation. In this pseudoequatorial orientation, the methyl group induces significant steric strain due to its proximity to the fluorenyl moiety. Therefore this diastereoisomer is of a metastable nature. Metastable-**1** can release its steric strain through a thermally activated helix inversion. This thermal helix inversion converts metastable-**1** to stable-**1′** which is chemically identical to the initial configuration of stable-**1**. However, the motors upper half has undergone a 180 degrees unidirectional rotation with respect to its lower half. The motor is functionalized with long alkyl chains to ensure solubility in a wide range of solvents and no significant degradation was observed after several rotary cycles (see ESI†). The thermal helix inversion (THI) can be monitored easily *via* UV-Vis spectroscopy. In a recent study, the activation parameters of the thermal helix inversion of motor **1** in a series of alkanes have been determined.[36] The obtained values of the half-life of metastable-**1** at 20 °C range from 331 s in pentane to 555 s in dodecane. This time scale is long enough for accurate measurements while still allowing for a large number of solvents to be scanned in a reasonable amount of time. We have studied 50 solvents divided over 11 solvent groups, each of which was selected to elucidate the influence of a certain solvent property on the THI. Table 1 summarizes the results of the measurements. For 18 solvents and solvent mixtures a full Eyring plot has been constructed and the activation parameters are presented. For the other solvents and solvent mixtures the rate of the THI has been measured at 20 °C. For all solvents, the dynamic viscosity at room

Table 1 Rate of thermal helix inversion (THI) of metastable **1**, viscosity, molecular weight and activation parameters for the 50 solvents and solvent mixtures investigated[a]

Solvent	ln k	ln η	Mol. weight	$t_{1/2}$[b] (min)	$\Delta^{\ddagger}H^{\circ b}$ (kJ mol^{-1})	$\Delta^{\ddagger}S^{\circ b}$ (J K^{-1} mol^{-1})	$\Delta^{\ddagger}G^{\circ b}$ (kJ mol^{-1})
Pentane	−6.172	−1.475	72.15	5.52	74.0	−43.6	86.8
Hexane	−6.221	−1.172	86.18	5.80	76.0	−37.4	86.9
Heptane	−6.299	−0.8896	100.2	6.28	80.4	−22.9	87.1
Octane	−6.388	−0.6127	114.2	6.87	76.0	−38.8	87.3
Nonane	−6.454	−0.3401	128.2	7.33	80.3	−24.6	87.5
Decane	−6.514	−0.09047	142.3	7.80	82.7	−17.0	87.6
Undecane	−6.603	0.1766	156.3	8.52	83.3	−15.6	87.9
Dodecane	−6.686	0.4069	170.3	9.25	80.6	−25.6	88.0
Dichloromethane	−6.386	−0.823	84.93	6.77	79.0	−28.5	87.3
Acetonitrile	−6.511	−1.017	41.05	7.72	84.6	−10.5	87.6
Methanol	−6.844	−0.4974	32.04	10.9	79.1	−32.0	88.4
10% glycerol in methanol	−6.953	−0.1859	34.28	12.1			
20% glycerol in methanol	−7.075	0.1912	36.85	13.7			
30% glycerol in methanol	−7.221	0.6223	39.83	15.8			
40% glycerol in methanol	−7.366	1.140	43.35	18.3			
50% glycerol in methanol	−7.615	1.757	47.54	23.3	87.4	−9.9	90.3
15% glycol in methanol	−6.998	−0.1612	34.55	12.6			
30% glycol in methanol	−7.095	0.2499	37.48	13.9			
40% glycol in methanol	−7.224	0.5570	39.73	15.9	83.0	−21.7	89.4
50% glycol in methanol	−7.372	0.8727	42.26	18.4			
Ethanol	−6.984	0.1868	46.07	12.4	81.1	−26.4	88.8
1-Propanol	−6.975	0.7931	60.10	12.4			
1-Butanol	−6.883	1.089	74.12	11.3			
1-Pentanol	−6.882	1.425	88.15	11.3			
1-Hexanol	−6.929	1.697	102.2	11.8			
1-Heptanol	−6.981	1.988	116.2	12.4			
1-Octanol	−7.002	2.178	130.2	12.7			
1-Nonanol	−7.120	2.548	144.3	14.3			
Benzene	−6.869	−0.4246	78.11	11.1	85.6	−9.94	88.5
Toluene	−6.851	−0.5240	92.14	10.9			
Ethylbenzene	−6.843	−0.3943	106.2	10.8			
Butylbenzene	−6.874	0.05552	134.2	11.2			
Hexylbenzene	−6.944	0.5331	162.3	12.0			
Octylbenzene	−7.034	0.9579	190.3	13.1	87.5	−4.88	88.9
Dodecylbenzene	−7.240	1.721	246.4	16.1			
para-Xylene	−6.856	−0.4349	106.2	11.0			
Diethylbenzene	−6.941	−0.1555	134.2	12.0	83.7	−17.0	88.7
Dibutylbenzene	−7.080	0.8901	190.3	13.7	88.8	−0.676	89.0
Anisole	−7.074	0.1028	108.1	13.7			
Benzonitrile	−6.307	0.3231	103.0	6.33			
Anisol/benzonitrile	−6.586	0.1673	105.5	8.37			
Methyl benzoate	−7.159	0.7277	136.2	14.9			
Cyclopentane	−6.421	−0.8461	70.10	7.10			
Cyclohexane	−6.486	−0.03315	84.16	7.57			
Cycloheptane	−6.524	0.4036	98.19	7.87			
Cyclooctane	−6.634	0.9245	112.2	8.78			
Isopentane	−6.060	−1.473	72.15	4.95			
Neohexane	−6.248	−1.008	86.17	5.97			
Methanol-d_4	−6.903	−0.4195	36.07	11.5			
Methanol-d_1	−6.854	−0.4952	33.05	11.0			

[a] For all recorded data and their derived parameters error margins were determined which can be found in the ESI. [b] At 20 °C and ambient pressure.

temperature has been determined in triplo using an Ubbelohde viscometer (see ESI†).

Polar solvents

Following the series of alkanes previously investigated, our initial investigations aimed at polar solvents. Fig. 1 shows the natural log of the rate of the THI at 20 °C, *versus* the natural log of the dynamic viscosity at the same temperature for several solvents. The black squares represent a series of alkanes, starting from pentane (top left) to dodecane (bottom right). As free volume theory predicts, these points form a straight line (R^2 = 0.994, Pearson's r = −0.997, see ESI†).[25] A detailed analysis of these results can be found in our earlier work (α° = 0.275 and β° = −6.55).[36] § The blue triangles represent mixtures of methanol and glycerol, starting from pure methanol (top left) to 50 wt% glycerol in methanol (bottom right). Because the dipole moments of methanol and glycerol are so similar (resp. 2.87 D and 2.56 D),[37]

§ Standard state (°) equals room temperature (20 °C) and atmospheric pressure (1 atm).

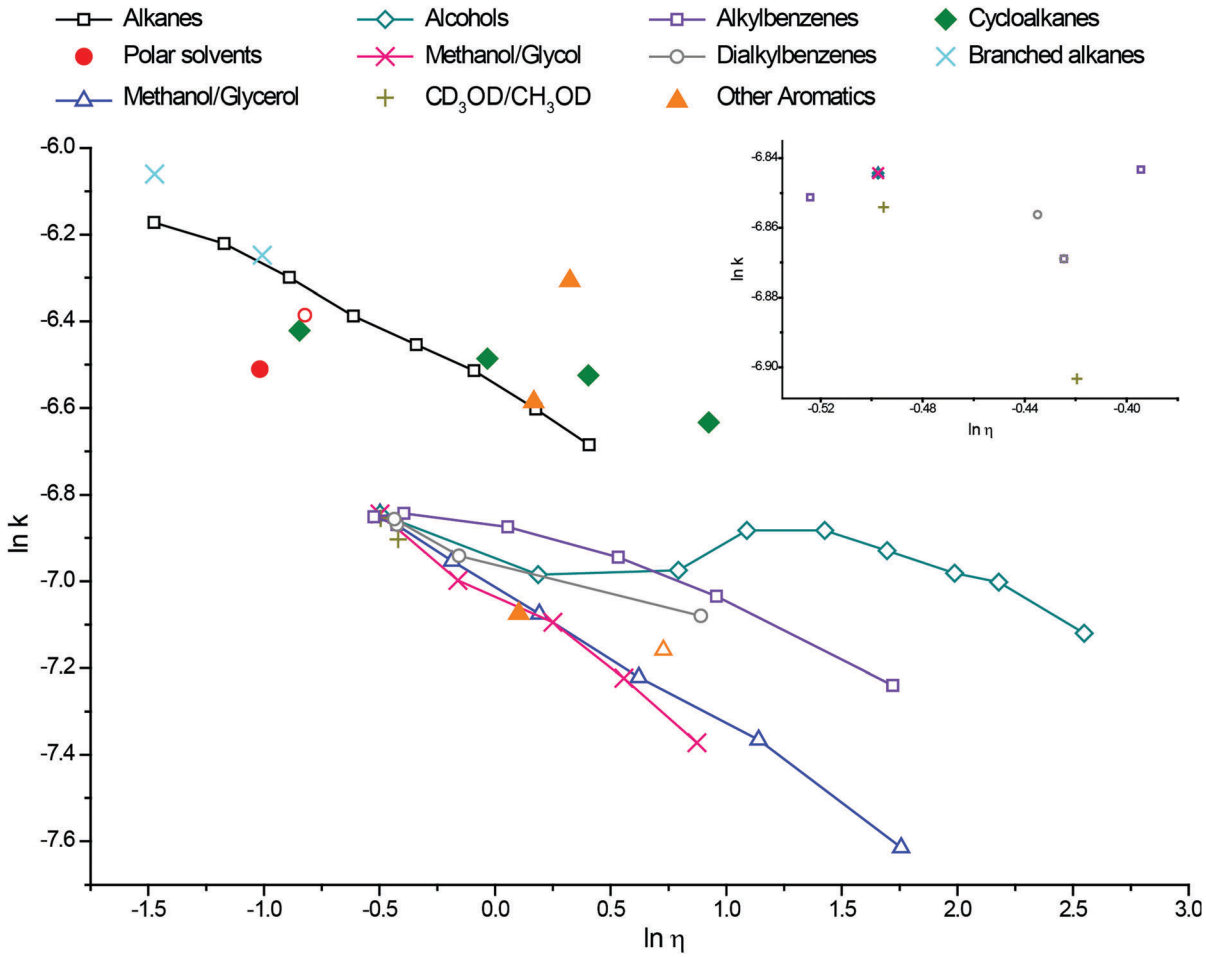

Fig. 1 ln *k* *versus* ln η for a series of alkanes (black squares), alcohols (turquoise diamonds), methanol/glycerol mixtures (blue triangles), methanol/glycol mixtures (pink crosses), monoalkyl aromatic solvents (grey circles), dialkyl aromatic solvents (purple squares), deuterated methanols (green pluses), polar solvents (red circles), electron rich or poor aromatic solvents (orange triangles), a series of cycloalkanes (green diamonds), branched alkanes (light blue crosses). For clarity, lines are given to guide the eye. A zoom-in of a crowded area of the graph is included in the top right corner.

this group of solvent mixtures represents a very close approximation of a perfectly homologous series of solvents with increasing viscosities and constant polarity (analogous to the homologous series of alkenes which also possesses constant polarity over increasing viscosity). The glycerol/methanol mixtures behave quite similar to the alkane series (R^2 = 0.998, Pearson's r = −0.999). Rate decreases when viscosity increases as predicted by Kramers theory for high-friction media (*i.e.* a liquid).[24] According to Schroeder, this linear relation indicates that the macroscopic viscosity is proportional to the microscopic friction around the solute.[21] However, the THI process of metastable-**1** in the glycerol/methanol series as a whole is significantly slower (has a larger negative β value) than in the alkane series (α° = 0.335 and β° = −7.01, *vs.* α° = 0.275 and β° = −6.55, respectively). Additionally, the rate of the THI of motor **1** was measured in dichloromethane and acetonitrile (Fig. 1, unfilled and filled red circle, respectively). Dichloromethane (dipole moment 1.14 D) lies more or less in the alkane series and acetonitrile (dipole moment 3.44 D), although significantly more polar than methanol and glycerol, lies only slightly above the extrapolated trend line for the glycerol/methanol series. Because there is no change in polarization during the isomerization process, these results are within our expectations.

Polarity is not the only difference between the alkane series and the glycerol/methanol series. Methanol and glycerol are excellent hydrogen bond donors and acceptors and their hydrogen bond forming ability per mass unit is very similar (methanol: 1 hydroxy group per 32.04 u, glycerol: 3 hydroxy groups per 92.09 u; equals 1 hydroxy group per 30.70 u). Therefore, the overall hydrogen bonding ability of the mixture does not change significantly upon increasing viscosity by varying the ratio of the components. This is in accordance with the linear increase of the natural log of k with an increasing natural log of the viscosity. Dichloromethane is both a poor hydrogen bond donor and acceptor, whereas acetonitrile is a fairly good hydrogen bond acceptor, which explains why in these solvents, the rate of the THI of motor **1** is lower than in the alkanes, but higher than in the glycerol/methanol series. A similar conclusion was reached by Benniston and Harriman, who report the rate of the thermal isomerization step of bis-oxonols in 26 different solvents.[30] They see a marked difference between

protic and aprotic polar solvents and deduce that hydrogen bonding to the bis-oxonol is responsible for the retardation. However, no mechanistic studies have been performed to confirm that solvent–solvent hydrogen bonding is not also partly responsible for the decrease in rate.

Motor **1** is a very apolar molecule and will have little or no hydrogen bonding itself to the solvent, yet hydrogen bonding appears to be the predominant factor in the difference in the rates of the THI. Therefore, it is implied in the current study that in this system, for the solvents studied thus far, solvent–solvent interactions rather than solvent–solute interactions have a much larger influence on the rate. In other words, the THI should be considered in a 'solvent–shell' type approach, as due to solvation, the solvent forms a shell around the molecule.[1,38] During the THI, the molecule is required to undergo a major rearrangement, which means that the solvent shell needs to rearrange as well. If intermolecular forces in the solvent are strong, for example due to hydrogen bonding, this rearrangement requires more energy input, thereby decelerating the motor rotation. These interactions will dominate the solvent effects upon thermal isomerization, since solvent–solute interactions appear to be minimal. This is in contrast with results found for azobenzenes, which are polar and therefore dominated by effects based solvent polarity.[28,29] In the current example, solvent–solute effects may still influence the rate. For example, weak hydrogen bonding of the solvent to the aromatic rings of motor **1** can be envisioned. However, since the overall dependence on viscosity is retained, these effects are of a much smaller magnitude than observed for more polar switches.

An additional set of solvents was measured in order to elucidate the differences between the solvent groups. Fig. 1 shows the results of these measurements. A series of *n*-alcohols confirms our assumptions regarding the importance of the hydrogen bonding ability, clearly exhibiting a non-linear trend (Fig. 1, turquoise diamonds, $R^2 = 0.412$, Pearson's $r = -0.642$). While rates in low-weight alcoholic solvents such as methanol ($\ln k = -6.84$) and ethanol ($\ln k = -6.98$) are significantly retarded compared to aliphatic solvents of similar viscosity (resp. octane ($\ln k = -6.39$) and undecane ($\ln k = -6.60$)), the alcohol series is converging towards the alkane series with increasing molecular weight. This is to be expected since large *n*-alcohols have an increasing aliphatic character with dispersion interactions dominating, and intermolecular hydrogen bonding is much reduced.

The data set of the glycerol/methanol mixtures was extended by measurements performed in glycol/methanol mixtures. Glycol has a very similar hydrogen bonding ability per mass unit (1 hydroxy group per 31.035 u) compared to methanol and therefore THI rates in these mixtures were expected to be similar to those in the glycerol/methanol series. As can be seen in Fig. 1 (pink crosses), the data indeed fits well on the glycerol/methanol trend line (combined methanol/glycol/glycerol series: $R^2 = 0.987$, Pearson's $r = -0.993$).

Polar solvents II and alcohols

The temperature dependence of the viscosities of methanol, glycol/methanol (40 wt%) and glycerol/methanol (50 wt%) were determined using a temperature regulated Ubbelohde viscometer (see ESI†). Using these parameters together with their activation parameters, the temperature dependence of α and β was derived (see ESI† for their temperature dependence parameters) which revealed β being higher for the methanol/glycol/glycerol series than for the alkane series over their entire temperature range. Deriving the viscosity-corrected activation parameters (see ESI†) clearly shows a comparable difference in activation energy between the two series which, under the overlapping experimental conditions (η = 0.6–2.2 cP, T = 0.0–20 °C), averages at 1.1 kJ mol^{-1} (ranging from 0.99–1.3 kJ mol^{-1}). This additional barrier in methanol/glycol/glycerol compared to the alkane group quantifies a hydrogen bond 'solvent-cage'. The indicated additional barrier (1.1 kJ mol^{-1}) suggests the 'breaking' of a very weak hydrogen bond or, more likely, merely a reorganization of the surrounding hydrogen bonds.[39]

If hydrogen bonding is indeed the reason that rates are much slower in the methanol/glycol/glycerol series than in the alkane series, changing the nature of the hydrogen bond might give an insight into the mechanism behind this rate retardation. Hydrogen and deuterium are electronically identical, and therefore it is often assumed that hydrogen bonds and deuterium bonds are identical.[40] However, their mass and therefore their vibrational energy are different. Calculations suggest that deuterium bonds can be slightly stronger than hydrogen bonds, with an energy difference of up to 1.3 kJ mol^{-1}.[40,41] The rate of the THI of motor **1** was therefore measured in both CD_3OD and CH_3OD (Fig. 1, green pluses). The result for CH_3OD was nearly identical to the result for methanol. The isomerization rate was slightly lower in CD_3OD, but this is expected due to its slightly lower viscosity. No additional conclusions can be obtained from these results, since a significant kinetic isotope effect appears absent.

Aromatic solvents

Subsequently aromatic solvents were investigated. Motor **1** has a large aromatic core, and therefore solvent–solute interactions other than those previously observed were expected. The rate was measured in two solvent series: alkylbenzenes (Fig. 1, purple squares, $R^2 = 0.922$, Pearson's $r = -0.960$), and *para*-dialkylbenzenes (Fig. 1, gray circles, $R^2 = 0.972$, Pearson's $r = -0.986$). Surprisingly, the rates in these solvents are much closer to those for the glycerol/methanol series than the alkane series. Benzene ($\ln k = -6.89$), toluene ($\ln k = -6.85$), ethylbenzene ($\ln k = -6.84$) and *para*-xylene ($\ln k = -6.86$) all behave almost identical to methanol ($\ln k = -6.84$). Just as seen for the alcohol series, towards longer alkyl chains both of these groups seem to converge to the alkane line which can be explained by the increasing aliphatic character of the solvents as molecular weight increases. Due to π–π stacking, intermolecular forces are expected to be much stronger in aromatic solvents than in aliphatic solvents, which is consistent with a solvent shell theory.[42] However, due to the aromatic nature of motor **1**, solvent–solute interactions could be of more importance in these aromatic solvents.

Aromatic solvents II, cycloalkanes and branched alkanes

To further investigate the influence of π–π interactions on the rate, the THI was measured in anisole, benzonitrile, and a 1 : 1 mixture of the two (Fig. 1, filled orange triangles). These two solvents have a very similar viscosity but a very different electronic configuration. In benzonitrile ($\ln k = -6.31$) the metastable isomer has a much shorter half-life than in anisole ($\ln k = -7.07$), and in fact than in all other aromatic solvents. We have considered many explanations regarding the remarkably different behavior of motor **1** in benzonitrile. The most likely is the theory that there are more solvent–solute interactions in the aromatic solvents *i.e.* π–π interactions, and that the transition state of the isomerization process can therefore be affected more strongly by the solvent. In the transition state, the butyl chain on the upper half of motor **1** is compressed against the lower half of the motor,[36] leading to a temporary increase in electron density. Interaction with the electron poor benzonitrile would relieve some of this electron density, thereby stabilizing the transition state and increasing the reaction rate, which would explain the difference between benzonitrile and the relatively electron-rich anisole and alkylbenzenes. This explanation would indicate a combination of dipole moment and possibly other solvent effects, but only affecting the isomerization when π–π stacking can occur. Such complex interactions are outside the scope of this research, but would certainly warrant further investigations. As a control, a different electron-poor aromatic solvent, methyl benzoate (Fig. 1, unfilled orange triangle, $\ln k = -7.16$), was measured. The data are in line with the results from the other aromatic solvents, which might indicate that electron density on the aromatic ring is irrelevant to the THI, leaving benzonitrile a solitary, inexplicable outlier from the aromatic solvent trend line.

Finally, the rate of the THI of motor **1** was determined in several cyclic (green diamonds) and branched (cyan crosses) alkanes (Fig. 1). Of the branched alkanes, neohexane ($\ln k = -6.248$) lies on the alkane line. Isopentane ($\ln k = -6.060$) has a similar viscosity to pentane but lies above the line due to a slightly faster THI. Not much can be concluded regarding the α value based on 2 data points, but for the thermal isomerization of bis-oxonols Benniston and Harriman[30] find that the α value is very different for branched alkanols than for linear alkanols. However, they attribute this effect to steric blocking of the hydroxy group. The deviation of isopentane from the alkane line might simply be a result of weaker van der Waals interactions within the solvent, as is apparent from the difference in cohesive energy density between isopentane (45.6 J cm^{-3}) and *n*-pentane (47.7 J cm^{-3}).[43] This could lead to a less dense solvent shell and therefore a lower barrier for the THI.

The cycloalkanes (Fig. 1, green diamonds, $R^2 = 0.930$, Pearson's $r = -0.965$), ranging from cyclopentane to cyclooctane, lie in the same region as the linear alkanes. This solvent group is not expected to have a linear trend. The smallest cycloalkane (cyclopentane) is very rigid, but with every methylene expansion the ring increases significantly in flexibility, *i.e.* degrees of freedom. Therefore, it seems likely that much larger cycloalkanes would ultimately behave as linear alkanes, whereas the small rings might exhibit a different behavior. Cyclopentane ($\ln k = -6.421$) for example, lies below the alkane line. Analogous to isopentane, the rate might in this case be lower than expected based on viscosity due to the highly rigid structure of cyclopentane, which could lead to a relatively tightly ordered solvent shell.

Correlation to various solvent effects

While viscosity and possibly hydrogen bonding and π–π interactions in the solvent explain most of the general trends observed in the graphs above, there are clearly other solvent effects that influence the rate of the THI. In an effort to elucidate these effects, the rate of the THI has been compared to 8 solvent parameters:[43–48] the Kamlet–Taft parameters for the hydrogen bond donating and accepting ability (α and β, respectively), two different polarity scales (π^* and $E_T(30)$), the dielectric constant ε, the surface tension (ST), the cohesive energy density (c.e.d.) and the diffusion coefficients D of motor **1**. The diffusion coefficients have been measured by DOSY-NMR (see ESI†), while the other solvent parameters were obtained from the literature. The combined data are summarized in Table 2.¶

Fig. 2 shows $\ln k$ for the THI of motor **1** plotted against the eight solvent parameters. These parameters reflect solvent properties that might back up the theory regarding the importance of hydrogen bonding and/or π–π interactions, and on the other hand shed light on the unexplained behavior that has been observed in several solvents. The parameters are not known for the glycerol/methanol and glycol/methanol mixtures used. However, comparison with other solvent groups might give some useful insight. A statistical analysis was performed on the datasets to avoid any biased interpretation (for details see ESI†). Where the Pearson correlation coefficient (r) is appropriate to evaluate the linear relationship between $\ln k$ and $\ln \eta$, it is not expected *a priori* of the other datasets to be linear. Therefore, the Spearman's rank correlation coefficient (ρ) was used to assess the presence of a monotonic relationship between the rate and the different solvent parameters. For example, the individual solvent groups exhibited strong linear relationships, indicated by very high Pearson correlations ($r > 0.95$ for all solvent groups except linear alcohols). However, when $\ln k$ *vs.* $\ln \eta$ is assessed as a whole, its linear relationship is less evident ($r = -0.689$). Nonetheless, the complete dataset does exhibit a significant strong monotonic relationship ($\rho = -0.728$).

Fig. 2a–c show 3 different parameters related to polarity. In Fig. 2a this is π^*, a polarity scale based on solvatochromism.[49] This scale is based on several dyes and gives a measure of the extent to which a solvent stabilizes ionic or polar solutes.

¶ These solvent parameters are not available for the glycerol/methanol, glycol/methanol and anisole/benzonitrile mixtures and could also not be found for cycloheptane, 1-heptanol, dodecylbenzene, neohexane and the deuterated solvents.

Table 2 8 different solvent parameters[a] of 33 solvents, plus the symbols used to depict the solvents in Fig. 2

Solvent	Symbol	ln k	π^{*}[44,45]	ε[46]	$E_T(30)$[46]	α[44,45]	β[44,45]	ST[47] (mN m^{-1})	D	c.e.d.[43,48] (J cm^{-3})
Pentane	■	−6.172	−0.08	1.84	30.9	0	0	16.1	17.93	47.7
Hexane	■	−6.221	−0.08	1.89	30.9	0	0	18.4		52.8
Heptane	■	−6.299	−0.08	1.94	30.9	0	0	21.1	11.00	56.3
Octane	■	−6.388	0.01	1.95	31	0	0	21.6		56.9
Nonane	■	−6.454		1.97	30.8			22.9		
Decane	■	−6.514	0.03	1.99	30.8	0	0	23.8		59.9
Undecane	■	−6.603						24.7		
Dodecane	■	−6.686	0.05	2.10	31	0	0	24.5	2.500	61.2
Dichloromethane	○	−6.386	0.82	9.02	40.7	0.13	0.10	27.8	11.28	97.5
Acetonitrile	●	−6.511	0.75	36.0	45.6	0.19	0.31	29.3		143
Methanol	◆	−6.844	0.60	33.6	55.4	0.93	0.62	22.5	8.719	204
Ethanol	◆	−6.984	0.54	25.0	51.8	0.83	0.77	22.4		168
1-Propanol	◆	−6.975	0.48	21.5	50.5	0.76	0.84	23.7		143
1-Butanol	◆	−6.883	0.47	18.4	49.7	0.79	0.88	25.4		122
1-Pentanol	◆	−6.882	0.40	15.8	49.3	0.84	0.86	25.8	1.386	
1-Hexanol	◆	−6.929	0.40	14.4	48.9	0.8	0.84	26.2		
1-Octanol	◆	−7.002	0.40	10.3	48.3	0.77	0.81	27.5		
1-Nonanol	◆	−7.120						28.3	0.425	
Benzene	■	−6.869	0.59	2.40	34.3	0	0.10	28.9	7.427	84.1
Toluene	■	−6.851	0.54	2.43	33.9	0	0.11	28.5	7.425	79.3
Ethylbenzene	■	−6.843						29.3		76.3
Butylbenzene	■	−6.874						29.2		
Hexylbenzene	■	−6.944						30.0		
Octylbenzene	■	−7.034							1.724	
para-Xylene	●	−6.856	0.43	2.27	33.1	0	0.12	28.6		79.2
Diethylbenzene	●	−6.941						29.0		
Dibutylbenzene	●	−7.080							2.032	
Anisole	▲	−7.074	0.73			0	0.32	35.7	4.339	
Benzonitrile	▲	−6.307	0.90	25.3	41.5	0	0.41	39.4	5.544	
Methyl benzoate	△	−7.159			38.1	0	0.39	37.8		
Cyclopentane	◆	−6.421						22.6		65.6
Cyclohexane	◆	−6.486	0	2.02	30.8	0	0	25.2		66.9
Cyclooctane	◆	−6.634						29.8		
Isopentane	×	−6.060								45.6

[a] Solvent parameters are the solvatochromism scales π^{*} and $E_T(30)$, the dielectric constant ε, the Kamlet–Taft parameters for hydrogen bonding ability (α) and hydrogen donating ability (β), the surface tension (ST), the diffusion constant D and the cohesive energy density (c.e.d.).

As motor is **1** neither ionic nor polar, any correlation found on this scale must be treated with caution. However, the position of the polar and some aromatic solvents on this scale relative to the alcohols indicates that there is no obvious relation between the π^{*} scale and ln k evident from a very weak Spearman's correlation (ρ = −0.345). In Fig. 2b, ln k is plotted against the dielectric constant, ε. This parameter reflects dipoles, polarizability and hydrogen bonding sites and is therefore a relevant measure of polarity. In this plot, the alcohol solvent group is again seen ranging from a high value on the x-axis (for methanol) to much lower values upon increasing the aliphatic tail length. All aliphatic and apolar aromatic solvents have a dielectric constant <5, and any other solvents are more or less randomly distributed over the graph (ρ = −0.571). Finally, Fig. 2c shows the $E_T(30)$ solvatochromism scale.[50] Out of the three polarity scales, this is the only one that plots dichloromethane and acetonitrile between the aliphatic solvents and the alcohols, where they would be expected if a correlation between $E_T(30)$ and ln k existed.

Otherwise, this plot looks very similar to Fig. 2a and b and exhibits a slightly better but still only moderate correlation (ρ = −0.629). Clearly the aliphatic and alcoholic groups stay well separated from each other on all polarity scales. However, within the alcoholic group or with respect to the other solvents under investigation, no clear correlation between the rate and solvent polarity has been observed. This is expected since we rationalized that the retardation in alcohols was specifically due to their hydrogen bond donating and accepting properties, while for aromatic solvents the retardation stems from their π–π solvent–solvent interaction. Both effects have a different origin than the polarity of the solvent.

In Fig. 2d and e the parameters plotted are the Kamlet–Taft parameters for hydrogen-bond donating ability and hydrogen

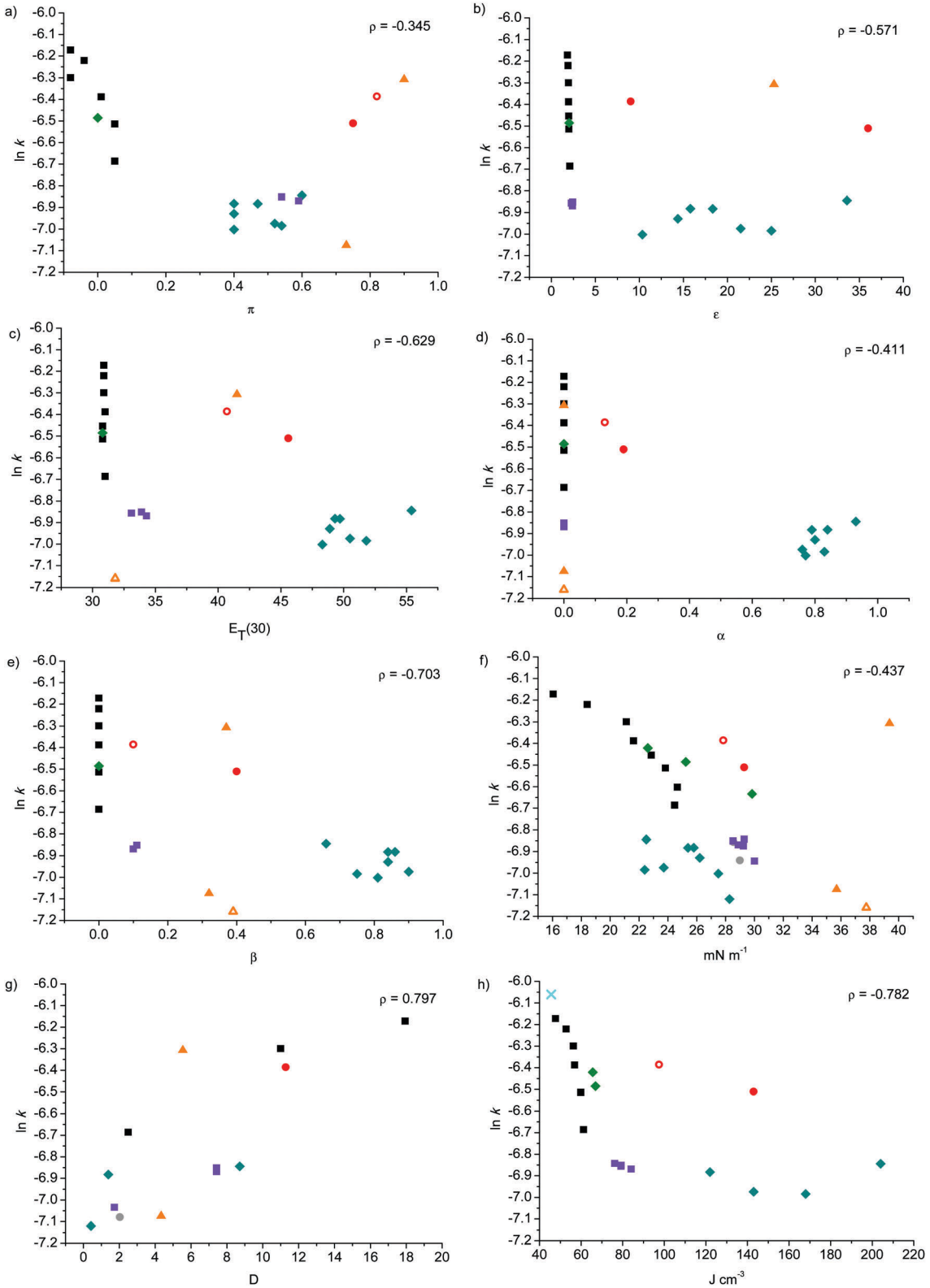

Fig. 2 Thermal helix inversion of 1; ln k plotted against 8 different solvent parameters. (a) The π^* polarity scale, (b) dielectric constant, (c) the $E_T(30)$ polarity scale, (d) the Kamlet–Taft parameter for hydrogen bond donating ability α, (e) the Kamlet–Taft parameter for hydrogen bond accepting ability β, (f) surface tension, (g) diffusion coefficient, (h) cohesive energy density. Spearman's rank correlation coefficient (ρ) indicated on each plot, for details see ESI.†

bond receiving ability, α and β, respectively, with scales ranging from 0 to 1.[51,52] For example, the aromatic solvents all have β values of up to 0.4 but α values of 0, ruling out any solvent-solvent hydrogen bonding interaction in aromatic solvents.

These parameters are 0 for all aliphatic solvents, but approach 1 for the alcohols. For α it is clear that a correlation is absent ($\rho = -0.411$), however, a noteworthy moderate correlation is observed for β ($\rho = -0.703$). This relatively high value may be attributed to weak hydrogen bonding of the solvent to the aromatic molecular motor. It has to be noted that this correlation is strongly influenced by the lack of distinction between the aliphatic solvents, which all possess an identical α and β value. Interestingly though, the Kamlet–Taft parameters of the alcohols decrease with an increasing alkyl length, mirroring the convergence of our alcohol trend line with the alkyl trend line (see Fig. 2). The polar solvents can be found about halfway between the alcohols and most other solvents on the Kamlet–Taft scales.

We expected a reasonable correlation for surface tension, it being strongly related to viscosity (Fig. 2f).[47] Surprisingly it provided a very weak and insignificant correlation ($\rho = -0.437$) with most data points spread around the mean. The most notable feature for this solvent property is the single significant outlier, benzonitrile. This solvent displayed a significant deviation in rate when compared to viscosity. Likewise, benzonitrile deviates when the natural logarithm of the rate is plotted against surface tension. However, in Fig. 1 this solvent deviates mainly form the aromatics while in Fig. 2f benzonitrile is an outlier from all other solvents, making the solvent an interesting subject for further studies.

Another property strongly related to viscosity is the diffusion coefficient (D).[53] Furthermore, this property is more attuned to the specific solvent–solute interaction since it is measured specifically for motor **1** by DOSY-NMR in several selected solvents (Fig. 2g).[54] Contrary to surface tension, the diffusion coefficient does exhibit a strong correlation with $\ln k$ ($\rho = -0.797$). This correlation is even stronger than that of viscosity with the rate, also when the viscosity dataset is reduced to the same size as that of the diffusivity (see ESI†). In addition, the Pearson correlation is high, which implies that the rate experiences a stronger linear relationship with the diffusion coefficient than with the viscosity. The high Pearson's r highlights the sensitivity of the diffusion coefficient with respect to solute–solvent interactions, which is to be expected from Kramer's theorem. Consequently, the diffusion coefficient is of the highest interest for future studies. It should be noted that also in this case the incongruity between benzonitrile and anisole persists with both solvents exhibiting similar diffusivities for **1**.

Finally, in Fig. 2h, $\ln k$ for selected solvents is plotted against the solvent cohesive energy density.[43,48] This parameter indicates the energy of vaporization, and is a direct reflection of the degree of van der Waals forces holding the molecules of the liquid together. Since rotation of the motor needs the solvent matrix to rearrange, which requires the van der Waals interactions between individual solvent molecules to be broken and reformed, this parameter could be very informative. This solvent parameters exhibits a significant and strong correlation ($\rho = -0.782$), even though it deviates from linearity, as can be seen in Fig. 2h, with acetonitrile and dichloromethane being the greatest outliers. This parameter does place the aromatic solvents roughly in the right position between the alkanes and alcohols, and due to the curvature it strongly differentiates between the groups. The lack of linearity and the limited amount of liquids for which the cohesive energy density is known makes the interpretation complex and warrants a deeper investigation of the relationship of the reaction rate to this solvent property.

The eight solvent properties (Table 2) under investigation were also examined for their viability as a correction factor for the viscosity with rate relationship (Fig. 1) which might reveal the property as a possible explanation for the deviation from linearity of the complete set of $\ln \eta$ *versus* $\ln k$. Of all properties, the cohesive energy density provided the largest improvement, however, none were found to fall within significant limits (p-value < 0.01, see ESI†). Therefore, from this analysis no additional information could be obtained regarding the differences in the solvent groups with respect to the viscosity dependence of their rates. An explanation might be obtained by the use of computational chemistry. In our previous paper we achieved a reasonable estimate for the THI barrier from DFT calculations and such calculations can be corrected using solvent models. However, the very subtle manner in which the solvents influence the rate for THI possibly require the inclusion of significant amounts of solvent molecules. Therefore, simulations using classical molecular dynamics might be the most appropriate tool to investigate the solvent shell surrounding the molecular motor as well as solvent–solute interactions. Such a study is beyond the scope of this paper but efforts towards this end are currently undertaken.

Conclusions

In conclusion, the rate of an apolar thermal unimolecular process has been measured in 50 different solvents and solvent mixtures. A large overall dependence of the rate on viscosity is clear, which follows our preliminary conclusions described in detail in earlier work.[36] This dependence is especially strong for groups of solvents of which other solvent properties remain consistent upon increasing viscosity. These groups exhibit a linear dependence of $\ln k$ on $\ln \eta$. However, the strength of this dependence differs between the series.

The relatively good fit between the overall data set and viscosity shows that solvent–solute interactions are small compared to those in azobenzenes and bis-oxonols This effect is presumably due to the apolar nature of motor **1** used as the solute. Therefore, the proposed model suggests that intermolecular forces in the solvent are the main reason behind this difference. The solvent shell around the solute needs to rearrange upon isomerization of motor **1**. When the van der Waals interactions between these solvent molecules are high, due to for example hydrogen bonding or π–π interactions, this requires more energy and therefore the thermal process is decelerated. Such effects have not been described previously for unimolecular thermal isomerizations, as rate change in polar and/or hydrogen bonding solutes is dominated by solvent–solute interactions, which are of a much larger magnitude. The natural

logarithm of the rate of rotation was plotted against 8 different solvent parameters. Statistical analysis provided a useful insight into the correlation of these solvent parameters with the rate of the THI. A moderate correlation was found with hydrogen bond donating ability of the solvent. However, the overall retained dependence on viscosity indicates only minor solvent–solute interactions. These results provide a markedly different insight in solvent effects on the isomerization process, since hydrogen bonding interactions are typically much stronger. As far as we are aware, no parameter scale based on π–π interactions exists. However, as the rate retardation in aromatic solvents could not be explained by any of the other parameters that were compared, it seems likely that these interactions are a relevant factor in the rate retardation of the THI of motor **1**. Furthermore, the best correlation was found with the diffusion coefficient and cohesive energy density. As the diffusion coefficient is strongly related to viscosity, these findings can be rationalized. However, the influence of cohesive energy density on the rate of the THI offers an interesting opportunity for further investigation. Additionally, dispersive interactions might play a significant role. In depth computational studies could shed light on such interactions.

Solvent effects comprise a vast range of different interactions, both among the solvent molecules and between solvent and solute. Hence, it is not surprising that the rate change of a unimolecular process in different solvents cannot be simply explained by one or two solvent parameters. It seems rather logical that such an effect is governed by a complex interplay between several distinct properties. It is tempting to draw conclusions based on trends observed within groups of similar solvents. Indeed, statistical analysis based on one solvent group could easily lead to a much higher correlation than any of the values reported in this work. However, we strive to give a comprehensive overview and show here not only the most extensive solvent scope performed so far on a thermal unimolecular reaction, but also the consideration of 9 different solvent parameters. Despite the complexity of the many possible combinations of solvent interactions, we have been able to identify a few parameters that significantly influence the rate of this apolar unimolecular thermal reaction. This knowledge will be highly relevant in the future design of molecular switches and motors, and the study of more complex dynamic systems.

Acknowledgements

Financial support from the Royal Netherlands Academy of Arts and Sciences (KNAW), the Netherlands Organization for Scientific Research (NWO-CW), the European Research Council (Advanced Investigator Grant, No. 227897 to B. L. F.) and the Ministry of Education, Culture and Science (Gravitation program 024.001.0035) is gratefully acknowledged. The authors would like to thank Pieter van der Meulen for useful advice and Prof. Giuseppe Graziano, Prof. Jan Engberts, Dr Alex de Vries and Dr Wiktor Szymanski for valuable discussions.

Notes and references

1 C. Reichardt and T. Welton, *Solvents and Solvent Effects in Organic Chemistry*, Wiley-VCH Verlag GmbH & Co. KGaA, Weinheim, FRG, 2010.
2 O. Tapia and J. Bertrán, *Solvent Effects and Chemical Reactivity*, Kluwer Academic Publishers, Dordrecht, 2002, vol. 17.
3 N. Menshutkin, *Z. Phys. Chem.*, 1890, **5**, 589.
4 E. Grunwald and S. Winstein, *J. Am. Chem. Soc.*, 1948, **70**, 846–854.
5 L. P. Hammett and A. J. Deyrup, *J. Am. Chem. Soc.*, 1932, **54**, 2721–2739.
6 E. D. Hughes and C. K. Ingold, *J. Chem. Soc.*, 1935, 244.
7 J. D. Moseley and P. M. Murray, *J. Chem. Technol. Biotechnol.*, 2014, **89**, 623–632.
8 J. Raeburn, C. Mendoza-Cuenca, B. N. Cattoz, M. A. Little, A. E. Terry, A. Zamith Cardoso, P. C. Griffiths and D. J. Adams, *Soft Matter*, 2015, **11**, 927–935.
9 J. L. Farmer, R. D. J. Froese, E. Lee-Ruff and M. G. Organ, *Chem. – Eur. J.*, 2015, **21**, 1888–1893.
10 G. Litwinienko, A. L. J. Beckwith and K. U. Ingold, *Chem. Soc. Rev.*, 2011, **40**, 2157.
11 L. Shuai and J. Luterbacher, *ChemSusChem*, 2016, **9**, 133–155.
12 A. Nitzan, *J. Chem. Phys.*, 1987, **86**, 2734.
13 G. N. Eyler, A. I. Cañizo, C. M. Mateo, E. E. Alvarez and L. F. R. Cafferata, *J. Org. Chem.*, 1999, **64**, 8457–8460.
14 D. L. Hasha, T. Eguchi and J. Jonas, *J. Am. Chem. Soc.*, 1982, **104**, 2290–2296.
15 Y. Hirata, Y. Kanemoto, T. Okada and T. Nomoto, *J. Mol. Liq.*, 1995, **65/66**, 421–424.
16 C. J. Tredwell, *J. Chem. Soc., Faraday Trans. 2*, 1980, **76**, 1627–1637.
17 W. Adam, M. Grüne, M. Diedering and A. V. Trofimov, *J. Am. Chem. Soc.*, 2001, **123**, 7109–7112.
18 W. Adam, V. Mart, C. Sahin and A. V Trofimov, *Chem. Phys. Lett.*, 2001, **340**, 26–32.
19 W. Adam and A. V. Trofimov, *Acc. Chem. Res.*, 2003, **36**, 571–579.
20 S. E. Greenough, M. D. Horbury, J. O. F. Thompson, G. M. Roberts, T. N. V Karsili, B. Marchetti, D. Townsend and V. G. Stavros, *Phys. Chem. Chem. Phys.*, 2014, **16**, 16187–16195.
21 J. Schroeder, *J. Phys.: Condens. Matter*, 1996, **8**, 9347–9387.
22 J. Schroeder, *Ber. Bunsen-Ges.*, 1991, **95**, 233–242.
23 M. Lee, A. J. Bain, P. J. McCarthy, C. H. Han, J. N. Haseltine, A. B. Smith III and R. M. Hochstrasser, *J. Chem. Phys.*, 1986, **85**, 4341–4347.
24 H. A. Kramers, *Physica*, 1940, **7**, 284–304.
25 D. Gegiou, K. A. Muszkat and E. Fischer, *J. Am. Chem. Soc.*, 1968, **90**, 12–18.
26 A. K. Doolittle, *J. Appl. Phys.*, 1951, **22**, 1471–1475.
27 K. M. Keery and G. R. Fleming, *Chem. Phys. Lett.*, 1982, **93**, 322–326.
28 K. Gille, H. Knoll and K. Quitzsch, *Int. J. Chem. Kinet.*, 1998, **31**, 337–350.

29 F. Serra and E. M. Terentjev, *Macromolecules*, 2008, **41**, 981–986.
30 A. C. Benniston and A. Harriman, *J. Chem. Soc., Faraday Trans.*, 1994, **90**, 2627–2634.
31 M. M. Pollard, P. V Wesenhagen, D. Pijper and B. L. Feringa, *Org. Biomol. Chem.*, 2008, **6**, 1605–1612.
32 R. A. van Delden, N. Koumura, A. Schoevaars, A. Meetsma and B. L. Feringa, *Org. Biomol. Chem.*, 2003, **1**, 33–35.
33 J. Chen, J. C. M. Kistemaker, J. Robertus and B. L. Feringa, *J. Am. Chem. Soc.*, 2014, **136**, 14924–14932.
34 J. Hicks, Z. Babarogic, M. Vandersall and K. B. Eisenthal, *Chem. Phys. Lett.*, 1985, **116**, 19–24.
35 M. Klok, L. P. B. M. Janssen, W. R. Browne and B. L. Feringa, *Faraday Discuss.*, 2009, **143**, 319.
36 J. C. M. Kistemaker, A. S. Lubbe, E. A. Bloemsma and B. L. Feringa, *ChemPhysChem*, 2016, **17**, 1819–1822.
37 R. Behrends, K. Fuchs, U. Kaatze, Y. Hayashi and Y. Feldman, *J. Chem. Phys.*, 2006, **124**, 144512.
38 R. Daudel, *Quantum Theory of Chemical Reactivity*, Springer, Netherlands, Dordrecht, 1973.
39 E. A. Anslyn and D. A. Dougherty, *Modern Physical Organic Chemistry*, University Science Books, Mill Valley, CA, 2006.
40 S. Scheiner and M. Čuma, *J. Am. Chem. Soc.*, 1996, **118**, 1511–1521.
41 M. Cuma and S. Scheiner, *J. Phys. Org. Chem.*, 1997, **10**, 383–395.
42 C. A. Hunter and J. K. M. Sanders, *J. Am. Chem. Soc.*, 1990, **112**, 5525–5534.
43 D. M. Koenhen and C. A. Smolders, *J. Appl. Polym. Sci.*, 1975, **19**, 1163–1179.
44 M. J. Kamlet, J.-L. M. Abboud, M. H. Abraham and R. W. Taft, *J. Org. Chem.*, 1983, **48**, 2877–2887.
45 Y. Marcus, *Chem. Soc. Rev.*, 1993, **22**, 409.
46 J. P. Cerón-Carrasco, D. Jacquemin, C. Laurence, A. Planchat, C. Reichardt and K. Sraïdi, *J. Phys. Org. Chem.*, 2014, **27**, 512–518.
47 J. J. Jasper, *J. Phys. Chem. Ref. Data*, 1972, **1**, 841.
48 J. Burke, *AIC B. Pap. Gr. Annu.*, 1984, **3**, 13–58.
49 M. J. Kamlet, J. L. Abboud and R. W. Taft, *J. Am. Chem. Soc.*, 1977, **99**, 6027–6038.
50 K. Dimroth, C. Reichardt, T. Siepmann and F. Bohlmann, *Ann. Chem.*, 1963, **661**, 1–37.
51 R. W. Taft and M. J. Kamlet, *J. Am. Chem. Soc.*, 1976, **98**, 2886–2894.
52 M. J. Kamlet and R. W. Taft, *J. Am. Chem. Soc.*, 1976, **98**, 377–383.
53 E. Cussler, *Diffusion Mass Transfer in Fluid Systems*, Cambridge University Press, New York, 3rd edn, 1997.
54 B. Antalek, *Concepts Magn. Reson., Part A*, 2002, **14**, 225–258.